

# 1 **Optimizing parameters for using the parallel auditory brainstem response** 2 **(pABR) to quickly estimate hearing thresholds**

3 Melissa J Polonenko<sup>1,3</sup>, ORCID: <https://orcid.org/0000-0003-1914-6117>

4 Ross K Maddox<sup>1,2,3</sup>, ORCID: <https://orcid.org/0000-0003-2668-0238>

5 <sup>1</sup> Department of Neuroscience, Del Monte Institute for Neuroscience, University of Rochester, NY, USA

6 <sup>2</sup> Department of Biomedical Engineering, University of Rochester, NY, USA

7 <sup>3</sup> Center for Visual Sciences, University of Rochester, NY, USA

8

9 Corresponding Author: Ross K Maddox, University of Rochester, Goergen Hall Box 270168, Rochester, NY  
10 15627, USA. [ross.maddox@rochester.edu](mailto:ross.maddox@rochester.edu)

11

12 **Keywords:** auditory brainstem response, evoked potentials, objective audiometry,  
13 electroencephalography, assessment

14

## 15 **Abbreviations:**

16 ABR – auditory brainstem response

17 ASSR – auditory steady-state response

18 pABR – parallel auditory brainstem response

19 dB peSPL – decibels peak-equivalent (baseline-to-peak) sound pressure level

20 dB nHL – decibels normal hearing level

21 PT – pure tone

22 RETSPL – reference equivalent threshold in sound pressure level

23

## 24 **Highlights**

- 25 • The pABR yields robust responses across stimulus rates and intensities.
- 26 • The optimal rate is 40 Hz, but using multiple rates may prove useful.
- 27 • The pABR shows some adaptation with increased stimulation rate.
- 28 • Extended analysis windows improve response detection for low stimulus frequencies.
- 29 • Behavioral thresholds subtly change across pABR rate, giving similar dB nHL values.

30

## 31 Abstract

32 Timely assessments are critical to providing early intervention and better hearing and spoken language  
33 outcomes for children with hearing loss. To facilitate faster diagnostic hearing assessments in infants, we  
34 developed the parallel auditory brainstem response (pABR), which presents randomly timed trains of tone  
35 pips at five frequencies to each ear simultaneously. We have shown that the pABR yields high-quality  
36 waveforms that are similar to the standard, single-frequency serial ABR but in a fraction of the recording  
37 time. While well-documented for standard ABRs, it is yet unknown how presentation rate and level interact  
38 to affect responses collected in parallel to random tone pip stimuli. Therefore, in this study we determined  
39 the optimal range of parameters for the pABR by recording responses across a range of six presentation  
40 rates, each at a low and high stimulus level. We show that a wide range of rates yields robust responses in  
41 under 15 minutes, but 40 Hz is the optimal singular presentation rate. Extending the analysis window to  
42 include later components of the response offers further time-saving advantages for the temporally broader  
43 responses to low frequency tone pips. Perceptual thresholds that subtly change across rate allow for a  
44 testing paradigm that easily transitions between rates, which may be useful for quickly estimating  
45 thresholds for different configurations of hearing loss. These optimized parameters facilitate expediency  
46 and effectiveness of the pABR to estimate hearing thresholds in a clinical setting.

## 47 1. Introduction

48 Early identification of hearing loss and timely intervention is important for promoting typical auditory  
49 development and spoken language acquisition (Ching et al., 2014; Cullington et al., 2017; May-Mederake,  
50 2012; Moeller, 2000; Niparko et al., 2010). Currently the gold standard for estimating hearing thresholds in  
51 young infants, and other individuals who do not provide reliable behavioral responses, involves serially  
52 measuring electrophysiological auditory brainstem responses (ABRs) to frequency-specific tone pip stimuli  
53 presented over a range of intensities to each ear separately (American Academy of Audiology, 2012; BC  
54 Early Hearing Program, 2012; NHS Newborn Hearing Screening Programme, 2013; Ontario Ministry of  
55 Children, Community and Social Services, 2018). These diagnostic ABRs can take a long time, and often  
56 yield incomplete information because the child cannot sleep or remain still long enough to obtain the  
57 necessary responses. Multiple visits to obtain a complete assessment delays treatment, carries additional  
58 costs and risk of attrition, adds stress to the family as they await clinical decisions, and burdens clinician  
59 times and resources. To address the time constraints of testing, we recently validated the new parallel ABR  
60 (pABR) as a viable method for facilitating faster recording of canonical ABR waveforms than traditional  
61 serial methods (Polonenko and Maddox, 2019). However, the optimal presentation rates across level for  
62 the pABR have yet to be established. In this paper we determined the optimal parameters for using the  
63 pABR to estimate hearing thresholds.

64 The pABR method uses time-saving strategies of simultaneous presentation of stimulus sequences at five  
65 frequencies to both ears and randomized stimulus timing sequences. Simultaneous presentation has been  
66 a successful tool used for estimating hearing thresholds with the auditory steady-state response (Luts et  
67 al., 2006; Slinger et al., 2018; Van Maanen and Stapells, 2010). While simultaneous presentation allows  
68 for multiple responses to be recorded, randomization allows for unrestricted analysis windows, affording  
69 higher stimulation rates and better estimates of the pre-stimulus noise (Burkard et al., 1990; Eysholdt and  
70 Schreiner, 1982; Polonenko and Maddox, 2019; Valderrama et al., 2016, 2014; Wang et al., 2013). These  
71 in turn provide better estimates of signal-to-noise ratio (SNR), a key metric that dictates testing time.  
72 However, the actual SNR gains achieved by higher rates become a trade-off between the reduction in  
73 noise and the shrinkage of response amplitudes due to neural adaptation at higher rates (e.g., Burkard et  
74 al., 1990; Burkard and Hecox, 1983; Chiappa et al., 1979; Don et al., 1977; Jiang et al., 2009).

75 The optimal range for stimulation rate across intensities is well studied for serial ABR measurement, but  
76 the effects of simultaneous stimulation across all frequencies with random timing are not obvious. Parallel  
77 presentation across frequency bands and ears may lead to cochlear excitation patterns that differ from the  
78 standard single-frequency ABR. Indeed, each frequency may act as a masker for the other frequencies,  
79 particularly at higher levels when there is more spread of activation along the cochlea. Preliminary

80 evidence for different interactions comes from the longer latencies and smaller amplitudes of wave V for  
81 the pABR than serial ABR, particularly at higher intensities and lower frequencies (Polonenko and Maddox,  
82 2019). Potential interactions that depend on both stimulus level and rate may result in optimal stimulus  
83 parameters for the pABR that differ from the standard ABR.

84 Clinical application of the pABR for threshold estimation will also depend on accurate calibration of the  
85 pABR stimuli. There are two considerations for calibration due to the short duration of tone pip stimuli. First,  
86 transient stimuli such as tone pips are physically calibrated in peak equivalent SPL (dB peSPL) by  
87 matching the amplitude of the tone pip to that of a 1000 Hz tone because the time constants of sound level  
88 meters are too long to adequately capture the level of the short stimuli (Laukli and Burkard, 2015). The  
89 amplitudes can be matched by the baseline-to-peak (peSPL) or peak-to-peak (ppeSPL) of the transient (for  
90 a discussion of the merits of both approaches see Laukli and Burkard, 2015). We chose to calibrate our  
91 pABR stimuli in dB peSPL since our stimuli were slightly asymmetric and for the ease of comparing to  
92 clicks and converting to other metrics such as peak SPL (pSPL). Second, transient stimuli are then  
93 psychoacoustically calibrated into units of dB normal hearing level (dB nHL) because perceptual sensitivity  
94 in dB peSPL (or dB SPL for tones) varies by frequency. Due to temporal integration, perceptual thresholds  
95 for brief stimuli such as tone pips are elevated compared to tones, and vary by pip duration and stimulation  
96 rate (Gorga et al., 1984; Gorga and Thornton, 1989; Sharma et al., 2003; Watson and Gengel, 1969).  
97 Therefore, the correction factors for converting thresholds in dB peSPL to the flattened curve of 0 dB nHL  
98 are specific to the tone pip parameters and transducers.

99 Therefore, in this study we investigated the effects of stimulus level and presentation rate on responses  
100 measured using the pABR method, with the goal of determining the optimal stimulus parameters and dB  
101 peSPL to dB nHL correction factors before evaluating clinical implementation of the pABR for threshold  
102 estimation. We show that the pABR yields responses with good SNR that can be recorded over a wide  
103 range of rates in reasonable recording times. Furthermore, we show that extending the analysis window to  
104 include additional components of the response offers advantages for response detection in many subjects,  
105 particularly for the broader responses to low frequency tone pips. Correction factors for perceptual  
106 thresholds were relatively similar (within 3.5–6 dB) across stimulation rates.

## 107 2. Methods

108 We completed two experiments. First, pABR electroencephalographic (EEG) responses were recorded to  
109 different rates and intensities. Second, behavioral thresholds were measured for pure tones and for the  
110 pABR stimuli at each rate to determine the correction factors that relate the stimulus level in dB peSPL to  
111 perceptual thresholds in dB nHL.

### 112 2.1. Subjects

113 EEG responses and psychoacoustic perceptual thresholds were collected in two separate experiments,  
114 each with a different set of 20 adults (13 females, 6 males, 1 non-identifying person for experiment 1; and  
115 11 females, 9 males for experiment 2). There was an additional subject recruited for perceptual threshold  
116 testing because one subject was excluded due to unreliable, sporadic thresholds from repeatedly falling  
117 asleep during behavioral testing. All subjects gave informed consent before participating in the  
118 experiments, which were done under protocols approved by the University of Rochester Institutional  
119 Review Board (#3866). The mean  $\pm$  SD (range) age was  $22.5 \pm 4.2$  (18–35) years for EEG testing, and  
120  $21.8 \pm 3.4$  (18–33) years for behavioral testing.

121 Normal hearing thresholds, defined as  $\leq 20$  dB HL, were confirmed at octave frequencies from 250–8000  
122 Hz. Tympanometry and otoscopy confirmed normal middle and outer ear function. Distortion product  
123 emission (DPOAE) testing confirmed normal outer hair cell function from 1–4 kHz, barring 2 subjects who  
124 had a DPOAE but poor SNR at 2 kHz in one of their ears. Most subjects also had DPOAEs at 500 Hz, but  
125 the noise floor was high and the DPOAE did not reach the 6 dB SNR criteria for one ear in 2 subjects and  
126 for both ears in 4 subjects.

## 127 2.2. pABR stimuli

128 Details of the pABR stimulus construction and method can be found in Polonenko and Maddox (2019).  
129 Briefly, stimuli to each ear comprised summed independent, randomly timed trains of Blackman windowed  
130 5-cycle cosine tone pips centered at octave frequencies from 500 to 8000 Hz. Individual tone pips had  
131 durations of 10, 5, 2.5, 1.25 and 0.625 ms for the frequencies 500, 1000, 2000, 4000 and 8000 Hz  
132 respectively. Thirty unique 1 s stereo epochs were created to ensure sufficient statistical independence  
133 between the pseudorandom Poisson processes controlling timing of the tone pip trains (Maddox and Lee,  
134 2018; Polonenko and Maddox, 2019). To create these tone pip trains, unit-height impulses were randomly  
135 inserted across 1 s and convolved with the tone pip. The number of impulses corresponded to the stimulus  
136 presentation rate. Polarity was randomly set to  $\pm 1$  so that half the tone pips were condensation and the  
137 other half rarefaction. For the EEG experiment, an inverted version of each of the 30 unique epochs was  
138 presented in sequence to counter-phase the stimuli to help mitigate stimulus artifact (i.e., Epoch A<sup>+</sup>, A<sup>-</sup>, B<sup>+</sup>,  
139 B<sup>-</sup>, etc, where A and B represent independent epochs and the superscript sign denotes the phase). For the  
140 behavioral experiment, a token from these 30 unique epochs was randomly chosen with replacement for  
141 each presentation of the stimulus.

142 The tone pip stimuli were calibrated to 80 dB peak-equivalent SPL (peSPL) by matching the amplitudes of  
143 the peak tone pip cosine component to the amplitude of a 1000 Hz sinusoid tone that read 80 dB SPL on a  
144 sound level meter (2240, Bruel & Kjaer) when played through an insert earphone (ER-2, Etymotic  
145 Research) attached to a 2-cc coupler (RA0038, G.R.A.S.). The other stimulus levels ( $L$ ) in dB peSPL were  
146 obtained by multiplying the reference-level tone pip by  $10^{(L-80)/20}$ . For the behavioral experiment, pure  
147 tones were created with amplitudes that were also calibrated to the same 80 dB SPL tone.

148 Stimuli were created at a sampling rate of 48 kHz and presented through ER-2 insert earphones connected  
149 to a sound card (Babyface Pro, RME, Haimhausen, Germany). For the EEG, the sound card was also  
150 connected to a headphone amplifier (HB7, Tucker Davis Technologies, Alachua, FL, USA), which sent an  
151 inverted stimulus to a second “dummy” set of earphones that had a blocked tube and was taped in the  
152 same orientation to the stimulus earphones. This setup further mitigated stimulus artifact by cancelling  
153 electromagnetic fields close to the transducers. The earphones were also hung from the ceiling by magnets  
154 to allow as much distance as possible between the transducers and EEG electrodes. Stimulus presentation  
155 was controlled by a python script using publicly available software at <https://github.com/LABSN/expyfun>  
156 (Larson et al., 2014). The sound card’s optical digital out was also used to send digital signals that  
157 precisely marked the beginning of each 1 s epoch, which were then converted to trigger pulses by a  
158 custom trigger box (modified from a design by the National Acoustic Laboratories, Sydney, NSW,  
159 Australia). These triggers were then sent to the EEG system in order to synchronize responses with stimuli.

## 160 2.3. EEG experiment

### 161 2.3.1. Stimulus conditions and EEG recording

162 We recorded responses in both ears to pABR stimulation with average presentation rates of 20, 40, 60, 80,  
163 100, and 120 Hz, each at intensities of 51 and 81 dB peSPL. For a single 2-hour recording session, this  
164 afforded 10 minutes for each of the 12 conditions, resulting in averaged responses comprised of 12,000  
165 (20 Hz rate) to 72,000 (120 Hz rate) repetitions. Conditions were interleaved to prevent changes in  
166 impedance, subject state, or EEG noise from affecting one condition more than the others.

167 Two-channel scalp potentials were recorded with BrainVision’s PyCorder software, using passive Ag/AgCl  
168 electrodes connected to two differential preamplifiers (BrainVision LLC, Greenboro, SC). In standard 10–20  
169 coordinates, the non-inverting (positive) electrode was positioned at FCz (just anterior of the vertex), the  
170 inverting (negative) electrodes at A1 and A2 (left and right earlobes), and the ground electrode at FPz  
171 (frontal pole). The non-inverting and ground electrodes were plugged into y-connectors that split between  
172 the two differential pre-amplifiers. Data were sampled at 10 kHz and high-pass filtered at 0.1 Hz. Triggers  
173 marked the beginning of each epoch rather than each individual tone pip stimulus for two reasons: 1) to  
174 avoid trigger overlap due to random stimulation of 10 tone pips (5 for each ear), and 2) to efficiently



175 analyze 1 s blocks of data in the frequency domain, which is mathematically equivalent to – but faster than  
176 – averaging responses to each individual tone pip. Participants reclined in a darkened sound treated  
177 audiometric booth during testing, and were encouraged to rest.

### 178 2.3.2. pABR response calculation

179 Further details can be found in Polonenko and Maddox (2019) but a brief description is provided below.  
180 Using the mne-python package (Gramfort et al., 2013), raw EEG was filtered offline from 30–2000 Hz using  
181 a first order causal Butterworth filter, and then notch-filtered at odd multiples of 60 Hz up to 2500 Hz to  
182 remove electrical line noise.

183 As mentioned above, triggers denoted the beginning of each 1 s epoch. This epoch, along with 500 ms  
184 before and after it was extracted for each trigger, giving 2 s of EEG data, denoted as  $y$ . This same EEG  
185 was used to derive responses for each of the 10 tone pips for that epoch. For each tone pip of frequency,  
186  $f$ , and ear,  $e$ , we took the rectified impulse sequence used to create the tone pip train – a unit-height  
187 impulse at the onset of each tone pip in the 1 s epoch – and zero-padded it with 500 ms before and after to  
188 give a 2 s impulse train with all the impulses in the center 1 s, which was denoted  $x_{f,e}$ . The response,  $w_{f,e}$   
189 was then calculated as the circular cross-correlation of the 2 s EEG and the 2 s zero-padded rectified pulse  
190 train, performed in the frequency domain as  $w_{f,e} = 1/n F^{-1} \{F\{x_{f,e}\}^* F\{y\}\}$  where  $F$  denotes the fast Fourier  
191 transform,  $F^{-1}$  its inverse,  $*$  denotes complex conjugation, and  $n$  the number of impulses in a sequence  
192 (e.g., 40 for the 40 Hz stimulation rate). Due to the circular nature of the cross-correlation, the time interval  
193  $[0, 500]$  ms was at the beginning of  $w_{f,e}$  and  $[-500, 0]$  ms at the end. Concatenating these two time  
194 intervals (i.e., discarding the middle 1 s of  $w_{f,e}$ ) gave the final response from  $[-500, 500]$  ms, where 0 ms  
195 denotes the onset of the tone pip. This was repeated for each of the 10 tone pips and for each of the two  
196 EEG channels for every epoch.

197 Average responses for each condition (level, rate, channel, ear, and tone pip frequency) were calculated by  
198 first weighting each epoch by the inverse variance of its pre-stimulus baseline from  $-480$  to  $-20$  ms relative  
199 to the summed pre-stimulus inverse variances of all epochs for that condition, and then summing across  
200 the weighted epochs. This method resembles Bayesian averaging (Elberling and Wahlgreen, 1985), but  
201 leverages the much longer 500 ms pre-stimulus baseline afforded by random stimulus timing. Using this  
202 averaging method, very noisy epochs contribute much less to the grand average by assigning a weight  
203 close to zero. This avoids the need for rejecting epochs based on threshold criteria. Responses were also  
204 averaged across channels to reduce noise because we were not interested in ipsilateral versus  
205 contralateral differences for this paper. However, it would be easy to keep the two channels separate for  
206 clinical applications.

### 207 2.3.3. EEG data analysis

208 The primary objective of this paper was to determine the optimal rate for quickly obtaining waveforms for all  
209 10 tone pips. To achieve this, we: 1) compared the wave V latency (ms) and amplitude ( $\mu$ V) across  
210 conditions using linear mixed effect regression with rate and intensity fixed effects and a random intercept  
211 per subject; 2) quantified the response SNRs; and 3) estimated the recording time required for all  
212 responses in a rate-intensity combination to achieve 0 dB SNR. We chose a threshold of 0 dB SNR based  
213 on when waveforms became clearly identifiable and what we have done previously (Maddox and Lee,  
214 2018; Polonenko and Maddox, 2020, 2019). Of course, other dB SNR thresholds would change the  
215 estimated times to reach this criterion, but in a proportional way for each condition. Two analysis time  
216 windows were tested to determine SNR: a 10 ms window to include wave V of the ABR, and a 30 ms  
217 extended window to include wave V of the ABR and early components of the middle latency response  
218 (MLR).

219 The dB SNR of each averaged response (i.e., after 600 epochs, or 10 minutes) was estimated according to  
220 the formula:  $SNR_{600} = 10 \log_{10}[(\sigma_{S+N}^2 - \sigma_N^2) / \sigma_N^2]$  where  $\sigma_N^2$  was the variance of the noise calculated as the  
221 mean variance over 10 ms (ABR wave V window) or 30 ms (ABR/MLR extended window) intervals from

222 -480 to -20 ms, and  $\sigma^2_{S+N}$  was the variance of the signal and noise calculated as the variance in the  
223 respective 10 ms or 30 ms latency range starting at a lag that captures wave V for each tone pip's  
224 frequency: 10.5, 7.5, 6.5, 5.0, and 5.0 ms for 500, 1000, 2000, 4000 and 8000 Hz respectively (Polonenko  
225 and Maddox, 2019; Stapells, 2010). Then we standardized the SNR to a 1 minute (60 s) run:  $SNR_{60} =$   
226  $SN_{600} + 10\log_{10}(60 / 600)$ . From  $SNR_{60}$  we estimated the time-to-0 dB SNR as  $60 \times 10^{-SNR_{60} / 10}$ . This time  
227 was calculated for each tone pip, but the overall acquisition time for a condition is based on the slowest  
228 waveform, and as such, was calculated as the maximum time-to-0 dB of the 10 simultaneously acquired  
229 waveforms. Cumulative density functions were computed across subjects of time-to-0 dB for each tone pip  
230 in order to determine the optimal presentation rate – the rate at which 90% of subjects reached an SNR  $\geq$  0  
231 dB for all 10 tone pips in the shortest recording time.

232 The linear mixed effects regressions and their power analyses were performed using the lmer4, lmerTest  
233 and simR packages in R (Bates et al., 2015; Green and MacLeod, 2016; Kuznetsova et al., 2017; R Core  
234 Team, 2020). To calculate power, the likelihood ratio test was performed on 1000 Monte Carlo  
235 permutations of the response variables based on the fitted model.

## 236 2.4. Perceptual thresholds experiment

### 237 2.4.1. Stimulus conditions and psychoacoustics parameters

238 The 1 s stimulus tokens used for EEG were also used for determining perceptual thresholds for dB nHL  
239 correction factors. However, the tone pip trains were not presented in parallel but serial to determine the  
240 threshold for each tone pip frequency. In addition to the tone pip stimuli, we measured thresholds for 1 s  
241 cosine pure tones at each frequency, which were calibrated using the same 1000 Hz tone at 80 dB SPL  
242 that was used to calibrate the pABR tone pips. The tones had raised cosine window edges set to 35 ms,  
243 which was within the American National Standards Institute (ANSI) S3.6-2010 rise/fall standards and  
244 matched that of our audiometer used for hearing screening.

245 During the behavioral task, subjects sat in a sound treated audiometric booth, looked at a dark computer  
246 monitor screen with a central white fixation dot, and responded with keyboard presses when they heard the  
247 stimulus. Stimulus presentation time was jittered by a random number between 1 to 4 s. Perceptual  
248 thresholds were measured using an automated tracker based on the modified Hughson Westlake method  
249 (Carhart and Jerger, 1959), with a 5 dB base step size in a 2-down/1-up paradigm and a starting level of 40  
250 dB (pe)SPL. If there was no response for the starting level, then the level was increased in 20 dB steps  
251 until the subject responded or a maximum level of 85 dB (pe)SPL was reached. Threshold was defined as  
252 the level at which 2 out of 3 correct responses were given when the level of the stimulus was ascending. All  
253 70 threshold tracks were randomly presented over the course of the experiment (2 ears x 5 frequencies x 7  
254 rates, with 0 Hz rate representing tones). For each presentation of a pABR tone pip, a random token was  
255 chosen with replacement from the thirty unique 1 s tokens. Breaks of at least 15 s were provided after  
256 every 4 threshold tracks, and subjects chose when to continue after a break if they needed longer than 15  
257 s to rest.

### 258 2.4.2. Data analysis

259 Attentional state drifted in some subjects resulting in a few spuriously high thresholds. Thresholds were  
260 considered outliers and removed when the threshold to the pABR stimulus was >40 dB above that for the  
261 pure tone, and the track was confirmed to be poor and reflecting dozing (i.e., the intensity increased to 85  
262 dB peSPL with no response). Of 1,400 thresholds, 23 (1.6%) were removed and there was never more  
263 than 3 of 40 data points removed for a frequency-rate condition.

264 The reference values in dB nHL were calculated similarly to what has been done before (Gorga et al.,  
265 1993; Sharma et al., 2003; Stapells and Oates, 1997). The thresholds to pure tones were subtracted from  
266 the thresholds to the brief pABR stimuli to correct for temporal integration and the subject's own pure tone  
267 thresholds. These corrections were modeled using linear mixed effects regression with fixed effects of rate,  
268 logged frequency, and their 2-way interaction, as well as a random intercept for subject-ear. Then the

269 corrections derived from the model for each rate-frequency condition were converted to reference values to  
270 give 0 dB nHL by adding them to the HA-1 coupler reference equivalent threshold in SPL (RETSPL) for the  
271 ER-2 earphones (i.e., the conversion of SPL to audiometric zero).

### 272 3. Results

#### 273 3.1. The pABR yields canonical brainstem responses that characteristically show 274 adaptation at higher rates.

275 We recorded the pABR over a range of stimulation rates in 20 Hz steps and at two intensities. Figure 1  
276 shows the grand average waveforms for each of these conditions, and for each ear and tone pip frequency.  
277 Overall, morphology of the pABR responses resembled the canonical responses from traditional ABR  
278 methods, with lower frequency responses exhibiting a broader wave V than the higher frequencies.  
279 Although wave V is the primary focus of methods for estimating hearing thresholds, Figure 1 also shows  
280 that additional ABR waves I and III were clearly visible in the higher frequency responses across several  
281 presentation rates, especially at the higher intensity of 81 dB peSPL.

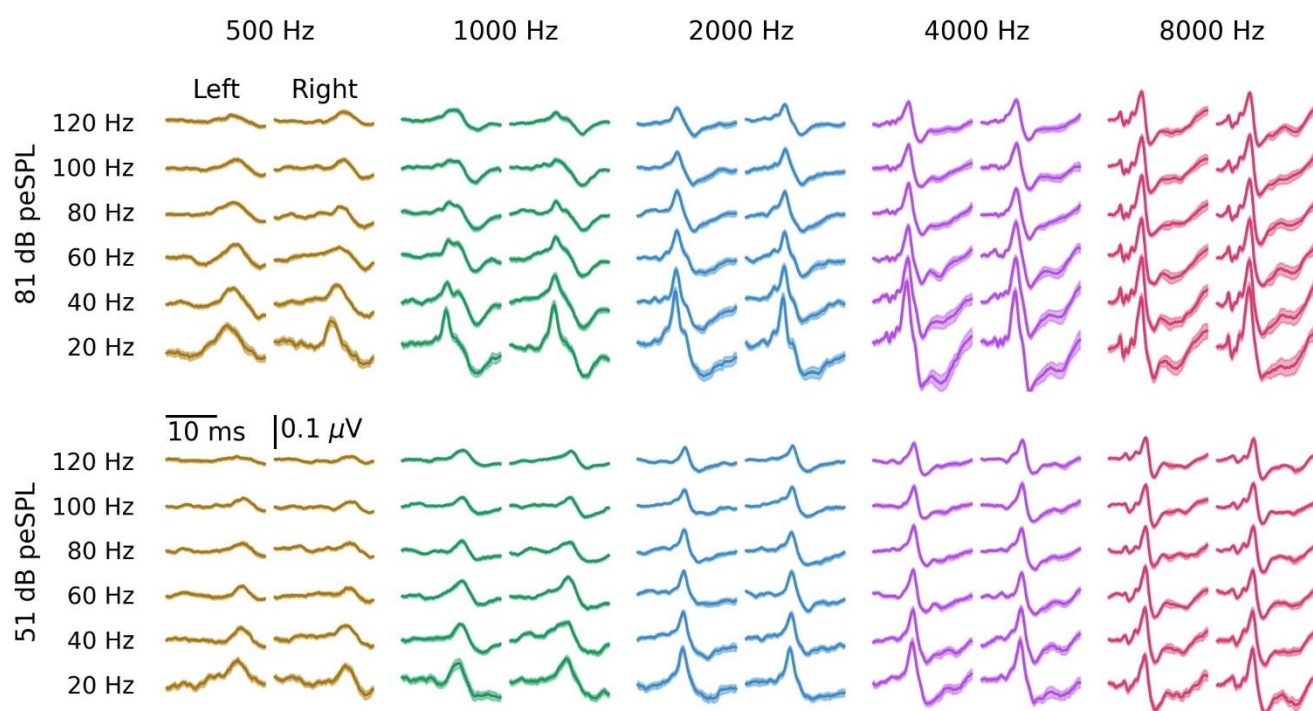


**Figure 1.** Grand average waveforms across stimulation rates and tone pip frequencies, plotted for both the left and right ears and for a high (top) and low (bottom) intensity. Areas show  $\pm 1$  SEM, computed across subjects. All responses are plotted over the interval 0 to 20 ms.

282 Waveforms were visually inspected and quantified for the presence, amplitude and latency of wave V.  
283 Amplitude was defined as the peak to following trough. All 2,400 responses were quantified by a trained  
284 audiologist (MJP), and the other author (RKM) quantified a subset of 720 responses (30%) from a random  
285 selection of 6 participants. The intraclass correlation coefficient for absolute agreement (ICC3) was  $\geq 0.81$   
286 for each frequency and measure (the lowest two ICC3 95% confidence intervals were 0.76–0.85 and 0.89–  
287 0.94 for 500 Hz latency and 1000 Hz amplitude respectively, all others were  $\geq 0.94$ ), indicating good  
288 agreement for chosen wave V peaks. There was not a clear wave V in 13 waveforms. These absent  
289 responses were for 500 Hz at the two highest stimulation rates of 100 Hz ( $n = 6$ ) and 120 Hz ( $n = 7$ ), and  
290 mostly for 51 dB peSPL (3 / 13 at 81 dB peSPL). For further analyses, the latencies of missing waves were  
291 removed and the amplitudes considered to be zero.



292 We modeled wave V latency (Figure 2A) and amplitude (Figure 2B) using linear mixed effects models, with  
 293 a random intercept for each subject and fixed factors of rate (in log units for amplitude due to the non-linear  
 294 relationship), intensity, ear, frequency in log units, and gender. We included the ear–frequency interaction,  
 295 as well as all 2-way and 3-way interactions between rate, intensity, and frequency. There was one subject  
 296 who did not identify as male or female and could not be included in the full model due to insufficient  
 297 numbers for a third gender category. Details of the full statistical models for latency and amplitude are  
 298 given in Supplemental Table 1A and 1B respectively. There was not a significant effect of gender for  
 299 latency ( $0.22 \pm 0.16$  ms,  $t(19) = 1.38$ ,  $p = 0.184$ , power = 0.29 [95% confidence interval: 0.26–0.32]), but  
 300 there was a trend that responses from female subjects were slightly larger ( $0.025 \pm 0.012$   $\mu$ V [95%  
 301 confidence interval = -0.001–0.049  $\mu$ V],  $t(19) = 2.05$ ,  $p = 0.054$ , power = 0.55 [95% confidence interval =  
 302 0.52–0.58]). To include all 20 subjects, we confirmed that the significant effects in the full model were  
 303 maintained in models excluding the non-significant fixed effect of gender, and the details of these statistical  
 304 models are found in Table 1. Wave V latency showed a difference between ears ( $p = 0.003$ ) but also a  
 305 significant ear–frequency interaction ( $p = 0.008$ ), indicating that responses for the right ear were faster for  
 306 lower frequencies (mean  $\pm$  SEM difference:  $0.28 \pm 0.07$  ms for 500 Hz) but similar for higher frequencies  
 307 ( $0.02 \pm 0.03$  ms difference for 8000 Hz). Consistent with our previous study (Polonenko and Maddox,  
 308 2019), there were also significant effects of intensity, frequency, and a significant intensity–frequency  
 309 interaction (all  $p < 0.01$ ), indicating that latency decreased with increasing frequency and increasing  
 310 intensity, and the effect of intensity was greater at lower frequencies. The slight increase in latency with  
 311 increasing rate was not significant ( $p = 0.875$ ), and there was no significant rate–intensity, rate–frequency,  
 312 or rate–intensity–frequency interactions (all  $p > 0.109$ ). Unlike latency, wave V amplitude showed no effect  
 313 of ear or an ear–frequency interaction (both  $p > 0.118$ ). Also consistent with our previous study (Polonenko  
 314 and Maddox, 2019), wave V amplitude increased with increasing intensity at a greater rate for higher  
 315 frequencies (intensity–frequency interaction,  $p < 0.001$ ). Here, we also showed that amplitude decreases  
 316 with increasing rate to a greater extent at higher intensities and higher frequencies (rate–intensity–  
 317 frequency interaction,  $p = 0.010$ ). There was an exception for 8000 Hz, which showed similar or smaller  
 318 amplitudes than 4000 Hz for the lower rates.

319

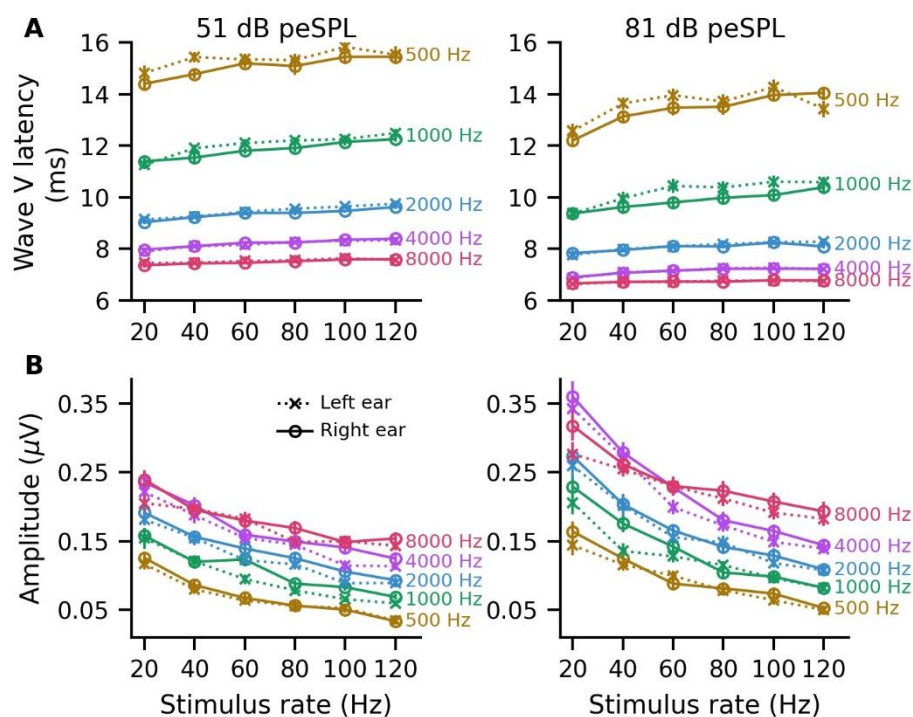


**Figure 2.** Mean wave V latency (A) and amplitude (B) as a function of stimulation rate at a low (left) and high (right) intensity. Stimulus frequency is indicated beside each line. Error bars (where large enough to be seen) indicate  $\pm 1$  SEM. Crosses joined by dotted lines indicate left ear responses and circles joined by solid lines indicate right ear responses.



**Table 1. Linear Mixed Effects Models for Wave V Latency and Amplitude**

Fixed Effect	Estimate	SE	df	t	p		Power (95% CI)
<b>A. Latency formula: <math>latency \sim rate + intensity + logfreq + ear + rate:intensity + rate:logfreq + intensity:logfreq + logfreq:ear + rate:intensity:logfreq + (1   subject)</math></b>							
Intercept [Left]	39.38	1.71	2375	23.05	< 0.001	***	1.00 (1.00, 1.00)
rate	0.00	0.02	2367	-0.16	0.875		0.04 (0.03, 0.05)
intensity	-0.18	0.03	2367	-7.13	< 0.001	***	1.00 (1.00, 1.00)
logfreq	-8.15	0.51	2367	15.90	< 0.001	***	1.00 (1.00, 1.00)
Ear [Right]	-0.99	0.33	2367	-2.98	0.003	**	0.84 (0.82, 0.86)
rate:intensity	0.00	0.00	2367	1.61	0.109		0.36 (0.33, 0.39)
rate:logfreq	0.00	0.01	2367	0.38	0.701		0.05 (0.04, 0.07)
intensity:logfreq	0.04	0.01	2367	5.33	< 0.001	***	1.00 (0.99, 1.00)
logfreq:ear [Right]	0.26	0.10	2367	2.64	0.008	**	0.75 (0.73, 0.78)
rate:intensity:logfreq	0.00	0.00	2367	-1.57	0.117		0.35 (0.32, 0.38)
<b>B. Amplitude formula: <math>amplitude \sim lograte + intensity + logfreq + ear + lograte:intensity + lograte:logfreq + intensity:logfreq + logfreq:ear + lograte:intensity:logfreq + (1   subject)</math></b>							
Intercept [Left]	0.26	0.20	2384	1.33	0.183		0.27 (0.24, 0.30)
lograte	-0.19	0.11	2380	-1.79	0.074	.	0.42 (0.39, 0.45)
intensity	-0.01	0.00	2380	-1.75	0.080	.	0.39 (0.36, 0.42)
logfreq	-0.06	0.06	2380	-1.01	0.312		0.18 (0.16, 0.21)
ear [Right]	-0.01	0.01	2380	-0.79	0.431		0.15 (0.13, 0.17)
lograte:intensity	0.00	0.00	2380	1.18	0.238		0.22 (0.20, 0.25)
lograte:logfreq	0.06	0.03	2380	1.73	0.083	.	0.41 (0.38, 0.44)
intensity:logfreq	0.00	0.00	2380	3.61	< 0.001	***	0.94 (0.93, 0.96)
logfreq:ear [Right]	0.01	0.00	2380	1.56	0.118		0.35 (0.32, 0.38)
lograte:intensity:logfreq	0.00	0.00	2380	-2.56	0.010	*	0.71 (0.68, 0.74)

Note: SE = standard error; logfreq =  $\log_{10}(\text{frequency})$ ; lograte =  $\log_{10}(\text{rate})$ ; .  $p < 0.1$ ; \*  $p < 0.05$ ; \*\*  $p < 0.01$ ; \*\*\*  $p < 0.001$

321

### 322 3.2. Acquisition times are fastest for a stimulation rate of 40 Hz

323 Next, we explored how the changes in amplitude with rate affect the time required for responses to reach  $\geq$   
 324 0 dB SNR using a 10 ms analysis window. We extrapolated to a maximum of 20 minutes, which was twice  
 325 our recording time but represented the minimum time required for serial collection of each response based  
 326 on our previous study (Polonenko and Maddox, 2019). To determine the optimal pABR rate for the majority  
 327 of subjects, the cumulative proportion of subjects was computed as a function of recording time. The  
 328 cumulative density functions (CDF) for the 40 Hz rate are shown in Figure 3A, and the CDFs for all rates  
 329 are provided in Supplemental Figure 1. Figure 3B shows the time to 0 dB SNR for 90% and 50% (median  
 330 time) of responses for each rate, which were taken from the CDFs.

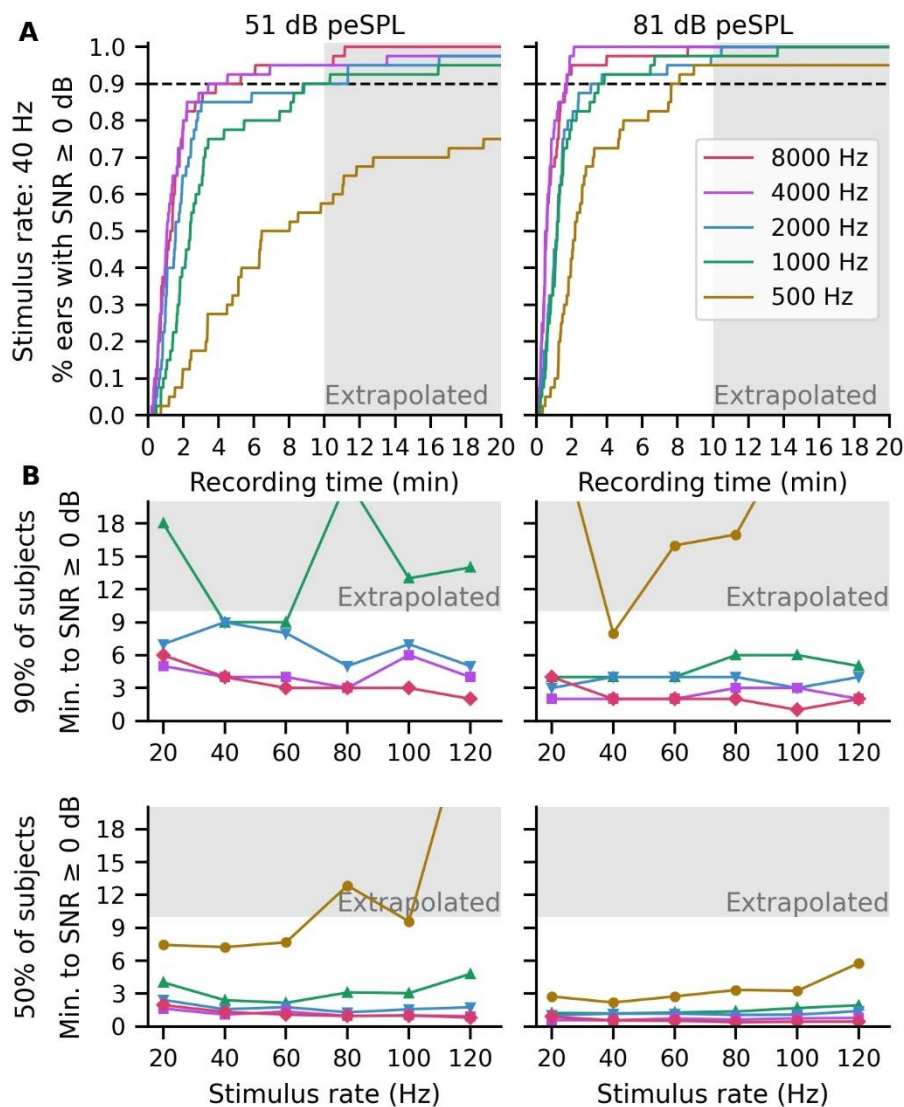


**Figure 3.** Acquisition times for waveforms to reach  $\geq 0$  dB SNR for a low (left) and high (right) presentation level for each tone pip frequency (indicated by line color). (A) The cumulative density function (CDF) is shown for the 40 Hz stimulation rate. From the CDF for each stimulation rate, the time for waveforms to reach  $\geq 0$  dB SNR in 90% and 50% of subjects (median) were calculated and displayed in (B). Shaded areas represent time estimations extrapolated past the 10-minute recording time.

332 Acquisition times were faster for the higher tone-pip frequencies and lower stimulation rates. Half the  
 333 subjects had all waveforms within 9.6 minutes for 51 dB peSPL and 3.5 minutes for 81 dB peSPL, except  
 334 for the 120 Hz rate at 81 dB peSPL (5.8 minutes) and for the 80 Hz and 120 Hz rates at 51 dB peSPL (12.9  
 335 and > 20 minutes respectively). In fact, for a 40 Hz stimulation rate the median time was 7.3 and 2.2  
 336 minutes for 51 and 81 dB peSPL. However, the acquisition time necessary for most subjects was limited by  
 337 the 500 Hz tone pip – the broadest and lowest-amplitude response. The estimated time for  $\geq 90\%$  of  
 338 subjects to reach 0 dB SNR for 2000–8000 Hz was  $\leq 9$  and 4 minutes for 51 and 81 dB peSPL  
 339 respectively. But for 500 Hz the acquisition time – and thus, the total time for the pABR – was > 20 minutes  
 340 for all rates at the lower intensity, and 7.7 minutes for 40 Hz but >15 minutes for the other rates at the  
 341 higher intensity. At the end of the 10-minute recording session, 48–72% of the 500 Hz responses reached  
 342 criterion at the lower intensity and 60–92% reached criterion at the higher intensity. Based on the 50% and  
 343 90% metrics, a 40 Hz stimulation rate appears optimal for ensuring the timeliest robust responses from  
 344 most subjects, although rates between 20–60 Hz required similar times for the mid and higher frequencies.

345 3.3. Extended analysis windows afforded by random timing improves SNR and saves  
346 time for low frequencies in some cases.

347 The random timing of the pABR allows for extending the analysis window to view more components of the  
348 evoked response. This advantage may improve SNR and acquisition estimates for the broader low  
349 frequency responses, which are present but vary less over 10 ms than the high frequency responses.  
350 Figure 4 shows the same responses from Figure 1 with the time window extended from 20 to 40 ms, which  
351 allows an analysis window of 30 ms for each tone pip frequency. With this extended window, the negative  
352 trough following wave V is now visible for the lower frequency responses (along with the higher frequency  
353 responses, which were visible with the shorter window), as well as the early components of middle latency  
354 response (MLR).

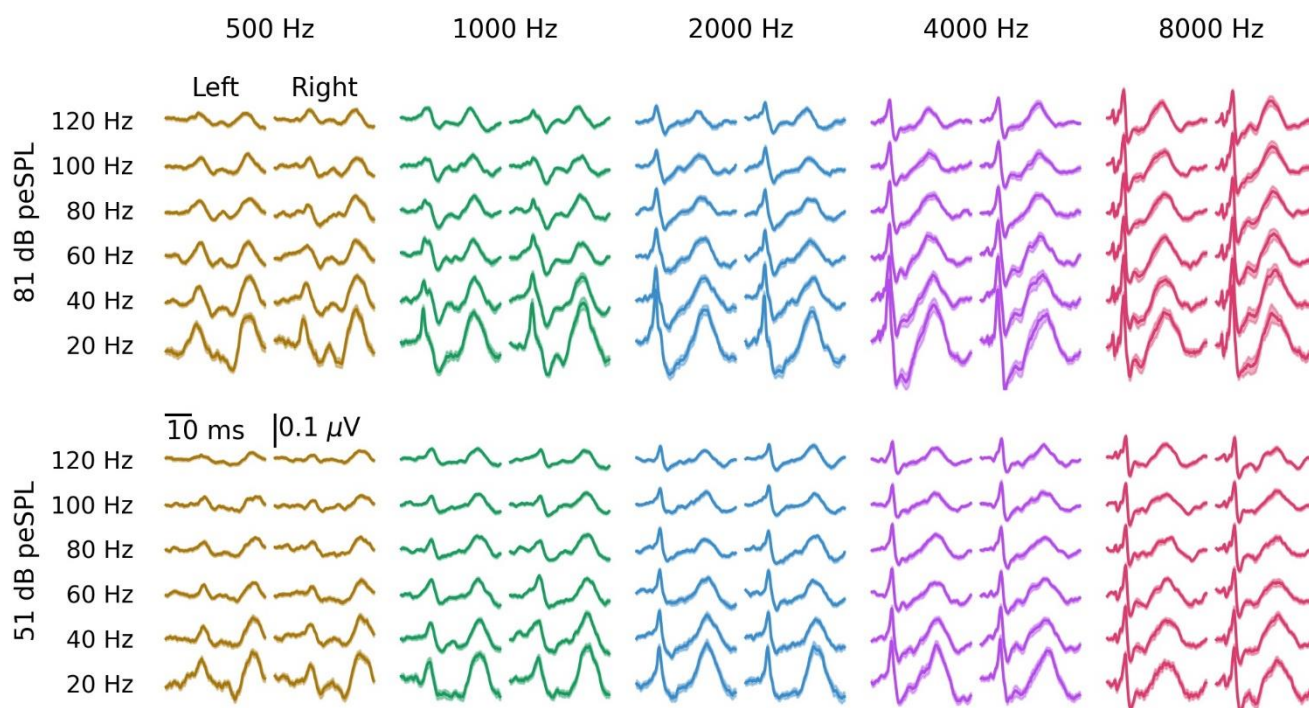


**Figure 4.** Grand average waveforms across stimulation rates and tone pip frequencies, plotted for both the left and right ears and for a high (top) and low (bottom) intensity. Areas show  $\pm 1$  SEM across subjects. All responses are plotted over the interval 0 to 40 ms.

355

356 Figure 5 compares the acquisition times for the low frequency tone-pips at low stimulation rates when using  
357 a 30 ms versus 10 ms window to estimate SNR. We focused on 20 and 40 Hz because these stimulation  
358 rates showed the best recording times with the 30 ms analysis window, as well as the greatest response  
359 variation over the extended window for 500 and 1000 Hz tone pips. For many subjects the 30 ms window  
360 provided similar or better estimates of SNR and acquisition times, especially for the 500 Hz tone pip. In  
361 Figure 5A, the CDFs for the 20 Hz stimulation rate began with a similar trajectory, but grew faster for the 30  
362 ms window (i.e., diverged from the curve for the 10 ms window) for recording times  $> 4$  minutes (at  $\sim 35\%$   
363 of ears) for 500 Hz and  $> 6$  minutes (at  $\sim 70\%$  ears) for 1000 Hz at 51 dB peSPL, and after  $\sim 5.5$  minutes for  
364 500 Hz (at  $\sim 72\%$  of ears) at 81 dB peSPL. The 1000 Hz CDF for the 10 ms window was higher than that  
365 for the 30 ms window at all times for 81 dB peSPL. This means that the 30 ms analysis window provided a  
366 time benefit for the  $\sim 65\%$  of 500 Hz waveforms and  $\sim 30\%$  of 1000 Hz waveforms that took longer than 4–6  
367 minutes to reach criterion SNR at the lower intensity level, but the 10 ms window was adequate for the  
368 quicker waveforms (i.e.,  $< 4$ –6 minutes) and for the most of the 1000 Hz tone pip waveforms at the higher  
369 intensity.



370

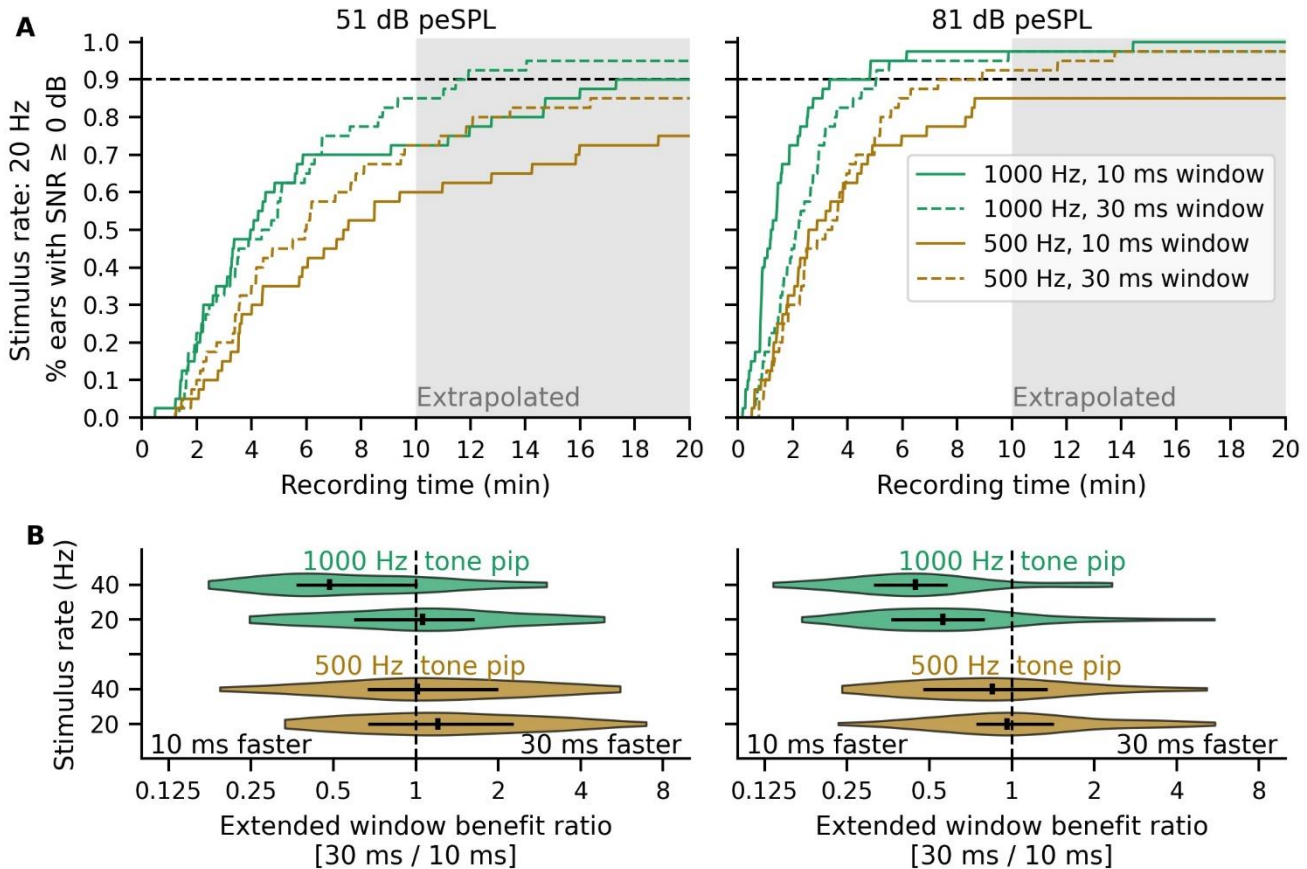


**Figure 5.** Extending the analysis window from 10 to 30 ms can improve response dB SNR and acquisition time for low frequency tone pips. (A) An example cumulative density function (CDF) is shown for the 20 Hz stimulation rate. Recording time required for waveforms to reach 0 dB SNR with a low (left) and high (right) presentation level for 500 and 1000 Hz tone pips when using an extended analysis window of 30 ms. Stimulus frequency is indicated by line color. (B) The distribution of extended window benefit ratios for using a 30 versus 10 ms analysis window. The horizontal black line indicates the interquartile range and the vertical solid black line denotes the median ratio. Ratios are on a log<sub>2</sub> scale, with ratios > 1 indicating a benefit to the 30 ms versus 10 ms window. The 10 ms window includes wave V of the ABR, and the extended 30 ms window also includes components of the middle latency response. The dashed line represents similar times to reach 0 dB SNR for both analysis windows.

371 Consistent with the CDFs, the distribution of extended window benefit ratios in Figure 5B suggest that the  
 372 30 ms analysis window provides a time benefit for the slower set of waveforms, with significant  
 373 improvements for some subjects. The greatest extended window benefit ratios for a 30 ms window  
 374 occurred for 500 Hz at 51 dB peSPL. Half the subjects had speedup ratios  $\geq 1$ , and for the “slowest 25%”  
 375 of subjects (i.e. 75<sup>th</sup> percentile and higher), the 30 ms window gave extended window benefit ratios of 2–7,  
 376 corresponding to 5.7–16.1 minutes saved by using a 30 ms window. At this intensity, the 75<sup>th</sup> percentile  
 377 extended window benefit ratios were < 1.6 (up to ~3 minutes saved) for 1000 Hz, but there were also some  
 378 cases that benefited from the 30 ms window by a ratio of 3-5, or up to 13–15 minutes saved. At the higher  
 379 intensity of 81 dB peSPL, there were faster or similar recording times for the 10 ms window in at least half  
 380 the subjects, with the median extended window benefit ratios  $\leq 1$  for both stimulus rates and tone pip  
 381 frequencies. However, the 30 ms window benefited about half the subjects for 500 Hz, and there were  
 382 significant improvements for some subjects for both 500 Hz and 1000 Hz. The 75<sup>th</sup> percentile extended  
 383 window benefit ratios were < 1 for 1000 Hz and < 1.4 for 500 Hz (up to 1.2 minutes saved by the 30 ms  
 384 window). Again, even for the high intensity, there were some extreme cases for whom the 30 ms provided  
 385 an extended window benefit ratio up to 5.5, corresponding to a maximum of 5 to 16.5 minutes saved. To  
 386 succinctly summarize the above, having the option to use a 30 ms window will speed the exam for some  
 387 patients.



388

### 389 3.4. Behavioral thresholds for pABR stimuli subtly change with rate

390 Having examined the effects of stimulation rate on the pABR responses and acquisition times, we next  
 391 compared perceptual thresholds to the pABR stimuli with those of pure tones to obtain normative values.  
 392 Figure 6A shows the perceptual thresholds in dB SPL for the pure tones and dB peSPL for the pABR  
 393 stimuli. Thresholds to the pure tones varied between -10 and 10 dB SPL and were elevated for the pABR  
 394 stimuli, as expected due to temporal integration of brief stimuli. Thresholds for the pABR stimuli subtly  
 395 decreased with increasing stimulation rate for each tone pip frequency. This pattern was similar for each  
 396 subject-ear, as indicated by the light colored lines. The difference between the thresholds to pABR stimuli  
 397 and pure tones ranged between 0 and 40 dB but were on average between 10 and 21 dB depending on  
 398 rate and tone pip frequency (Figure 6B).

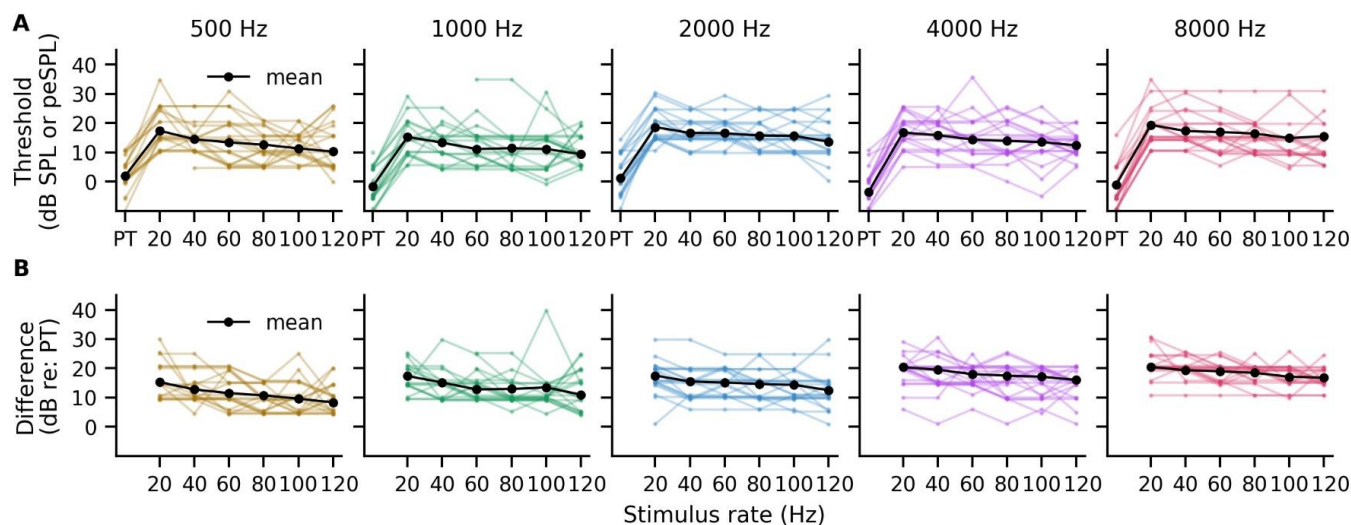


**Figure 6.** Perceptual thresholds show subtle changes across different stimulation rates. (A) Perception thresholds for pure tones (PT) and the pABR stimuli with different rates are shown for individuals (color) and the group mean (black). (B) The difference between thresholds to the pABR and pure tone stimuli. Individual colored lines are given a slight random vertical offset between  $\pm 1$  dB to make the individual data with similar thresholds easier to see.

399 Next, the normative values for 0 dB nHL were calculated. First, the difference in thresholds, or correction  
 400 factors, for the pABR stimuli (from Figure 6B) were modeled using linear mixed effects regression. Details  
 401 of the statistical model are provided in Table 2. As shown in Figure 7A, the threshold difference significantly  
 402 decreased with increasing stimulation rate ( $p = 0.004$ ) and increased with increasing frequency ( $p < 0.001$ ),  
 403 but there was not a significant interaction between rate and frequency ( $p = 0.085$ ). The mean difference in  
 404 correction factor between stimulation rates of 20 and 120 Hz ranged from 3.5 dB for the 500 Hz tone pip to  
 405 6.0 dB for the 8000 Hz tone pip. Second, the reference-equivalent thresholds in SPL (RETSPs) for our  
 406 ER-2 insert earphones were added to the correction factors to give the normative values for 0 dB nHL  
 407 (Figure 7B). The values from Figure 7 are also provided in Table 3 for ease of reference.

**Table 2.** Linear Mixed Effects Model for pABR Correction Values

Model formula:  $\text{correction} \sim \text{rate} + \text{logfreq} + \text{rate}:\text{logfreq} + (1 | \text{subject-ear})$

Fixed Effect	Estimate	SE	df	t	p	Power (95% CI)
Intercept	3.01	3.20	1162	0.94	0.348	0.14 (0.12, 0.16)
rate	-0.12	0.04	1138	-2.87	0.004	** 0.80 (0.77, 0.82)
logfreq	4.74	0.96	1138	4.97	< 0.001	*** 1.00 (0.99, 1.00)
rate:logfreq	0.02	0.01	1138	1.73	0.085	0.39 (0.36, 0.43)

Note: SE = standard error; logfreq =  $\log_{10}(\text{frequency})$ ; correction values = threshold differences for pABR tone pip versus pure tone; \*  $p < 0.05$ ; \*\*  $p < 0.01$ ; \*\*\*  $p < 0.001$

408

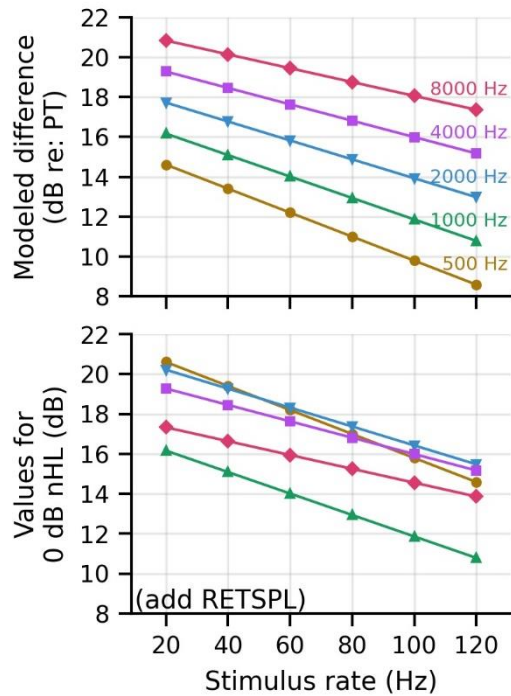


**Figure 7.** Correction factors for pABR stimuli. The modeled threshold differences, or correction factors, in (A) are added to the appropriate reference-equivalent threshold in SPL (RETSPL) for the transducer (in our study, ER-2 with HA-1 coupler) to give the normative values for audiometric zero (i.e., dB nHL) in (B). PT = pure tone

409

**Table 3.** Correction and normative values for converting pABR dB peSPL to 0 dB nHL

Tone pip	Stimulus rate					
	20 Hz	40 Hz	60 Hz	80 Hz	100 Hz	120 Hz
<i>Model-estimated correction factors (dB)</i>						
500 Hz	14.6	13.4	12.2	11.0	9.8	8.6
1000 Hz	16.2	15.1	14.0	12.9	11.9	10.8
2000 Hz	17.7	16.8	15.8	14.9	13.9	13.0
4000 Hz	19.3	18.5	17.6	16.8	16.0	15.2
8000 Hz	20.8	20.1	19.4	18.8	18.1	17.4
<i>ER-2 normative values for 0 dB nHL (dB)<sup>1</sup></i>						
500 Hz	20.6	19.4	18.2	17.0	15.8	14.6
1000 Hz	16.2	15.1	14.0	12.9	11.9	10.8
2000 Hz	20.2	19.3	18.3	17.4	16.4	15.5
4000 Hz	19.3	18.5	17.6	16.8	16.0	15.2
8000 Hz	17.3	16.6	15.9	15.2	14.6	13.9

<sup>1</sup>RETSPL for the ER-2 transducer (calibrated in an HA-1 coupler) was added to the model-estimated correction factors: 500 Hz = 6 dB, 1000 Hz = 0 dB, 2000 Hz = 2.5 dB, 4000 Hz = 0 dB, 8000 Hz = -3.5 Hz

410

411 With these normative values, the 51 and 81 dB peSPL intensities used to evoke the pABR responses  
 412 convert to a range from 30–35 and 60–65 dB dB nHL respectively for a 20 Hz stimulation rate to 36–40 and  
 413 66–70 dB nHL for 120 Hz rate. For the 40 Hz stimulation rate, 51 and 81 dB peSPL corresponded to 32–36  
 414 and 62–66 dB nHL respectively, with an average dB nHL across tone pip frequency of 33 and 63 dB nHL.

## 415 4. Discussion

416 Here, we describe how the pABR changes with stimulation rate and establish normative correction values  
417 for pABR levels based on perceptual thresholds. A wide range of rates yields robust responses in  
418 reasonable recording times for most subjects. For adults with normal hearing, the total recording time is  
419 limited by the broader component wave V of the waveforms for the low frequency tone pips. For some  
420 subjects with particularly broad responses, extending the analysis window improves response detection  
421 and the acquisition time necessary to reach SNR criterion. The perceptual thresholds to pABR stimuli  
422 subtly change with rate, giving a relatively similar set of correction factors to convert the level of the pABR  
423 stimuli from dB peSPL to nHL. Overall, the 40 Hz stimulation rate is the singular optimal rate, but in the  
424 clinic a range of rates may be useful for facilitating faster acquisition of elevated hearing thresholds across  
425 frequency.

426 Responses to pABR stimulation show adaptation to higher rates, both at a low and a high intensity. Even  
427 though the pABR uses random timing and simultaneous presentation of all 10 tone pips, wave V amplitude  
428 decreases with increasing frequency in a similar way to responses evoked by serially presented click  
429 stimuli (e.g., Burkard et al., 1990; Burkard and Hecox, 1983; Chiappa et al., 1979; Don et al., 1977; Jiang  
430 et al., 2009), but the latency minimally changes (Figure 2, Table 1, Supplemental Table 1). The benefit of  
431 higher rates is decreased noise, as variance reduces linearly with increasing number of stimuli. However,  
432 at some point adaptation limits this benefit by decreasing the response amplitude enough that SNR and  
433 response detection suffer. This trade-off can be seen in the estimates of recording time required to reach 0  
434 dB SNR. The acquisition times improve (i.e., become faster) or remain similar for rates up to either 60 or 80  
435 Hz – especially for the mid-to-high frequencies – and then lengthen again for the higher rates (Figure 3B)  
436 as the responses become smaller and broader (Figures 1, 4). When considering all tone pip frequencies at  
437 both intensities, the fastest recording times for most subjects is achieved with a 40 Hz stimulation rate – a  
438 rate that is consistently used in current clinical protocols (American Academy of Audiology, 2012; BC Early  
439 Hearing Program, 2012; Ontario Ministry of Children, Community and Social Services, 2018). However, the  
440 trade-off between adaptation and SNR is subtle for the pABR stimuli, especially depending on the tone pip  
441 of interest. If focusing on low frequency tone pips then the 20–40 Hz rates are optimal, but for tone pips  $\geq$   
442 2000 Hz, higher rates continue to improve acquisition times by a few minutes for most subjects (Figure 3).  
443 A few minutes represents valuable time when conducting diagnostic tests on infants, when the length of  
444 napping, and thus remaining testing time, is unknown. Furthermore, the effect of rate may not be as drastic  
445 for infants – amplitudes for click stimuli do not decrease as much for infants compared to adults, although  
446 they start off with a smaller amplitude for lower rates (Lasky, 1997, 1984). Therefore, despite adaptation, a  
447 method that utilizes a combination of rates may speed up the time required to estimate hearing thresholds  
448 that may differ across frequencies, and will need to be tested in the clinic and with infants.

449 Acquisition times are reasonable for the pABR stimuli, and can be supported by extending the analysis  
450 window to better capture broader responses in some subjects. For most subjects, an analysis window of 10  
451 ms adequately covers the wave V component (Figures 1, 5) and provides timely estimates to 0 dB SNR,  
452 with median total recording times for all 10 tone pips at most rates within 10 minutes for the lower intensity  
453 and within 4 minutes for a higher intensity (Figure 3). However, the recording time at a given level, at which  
454 the pABR yields responses for all frequencies in both ears, depends on the slowest response to emerge.  
455 For our adults with normal hearing, the broader 500 and 1000 Hz responses are the slowest – these two  
456 responses increase the median testing time for most rates from  $< 4$  minutes for the lower intensity and  $< 2$   
457 minutes for the higher intensity to  $< 10$  and  $< 4$  minutes respectively. These are still acceptable times to  
458 simultaneously collect 10 responses (Polonenko and Maddox, 2019), but there are cases where the  
459 recording times are much longer for the low frequency tone pips. The “slowest quartile” of subjects have  
460 testing times that are  $< 10$  minutes for 2–8 kHz tone pips but  $> 15$  minutes for the low frequency tone pips  
461 (Figures 3, 5). In the cases where the low-frequency tone pip responses are visible, but the time for  
462 reaching the criterion SNR is taking longer than 6–9 minutes, there can be a significant speedup benefit of  
463 5–16 minutes (corresponding to speedup ratios of 2–7) to using an extended analysis window that captures  
464 more of the broader response (Figure 4; Stapells and Oates, 1997). This longer analysis window which is

465 afforded by the random timing of the pABR and can be done for the same recording data, thereby not  
466 requiring extra recording runs/time. Next, the stimulation rate can be reduced to 20 Hz, which gives the  
467 most speedup advantage for detecting a response for 500 Hz at a lower intensity (Figure 5). This flexibility  
468 of using multiple analysis windows and stimulation rates gives another option in the toolkit that is easily  
469 implemented with the pABR.

470 Measurement time will also depend on hearing thresholds and implementation into a clinical setting. Time  
471 is limited by the 500 and 1000 Hz responses in the context of adults with normal hearing, but most hearing  
472 losses are more severe in the higher frequencies (e.g., Pittman and Stelmachowicz, 2003). When obtaining  
473 responses at higher intensities, the threshold for the lower tone pip frequencies will either be established  
474 already or a response confirmed as present at the higher intensity. Then the time will be limited by the SNR  
475 of the higher tone pip frequency responses. Response amplitudes tend to be more linear for hearing loss  
476 and for high frequencies, because high frequency responses do not suffer the same blurring together of  
477 tone pips or adaptation (shallower amplitude-rate slopes at a level closer to threshold | Figure 2; smaller  
478 changes in recording time in Figure 3). Both of these suggest that there may still be time-saving  
479 advantages of using higher rates when searching for elevated thresholds at higher frequencies. At the  
480 lower intensity of 51 dB peSPL, 90% of subjects reached criterion within 5 minutes for the 2–8 kHz tone  
481 pips, compared to 7–9 minutes for rates < 80 Hz. Using faster rates for higher frequencies may save  
482 valuable time and allow more intensities to be tested within a recording session, giving a more complete  
483 exam. Of course the actual acquisition times will depend on the stopping criteria and implementation in the  
484 clinic. Here we used 0 dB SNR, but the reported minutes will scale if that threshold is changed (doubling,  
485 e.g., if it is increased to 3 dB SNR). We will next evaluate the pABR in a clinical setting and determine the  
486 time to find thresholds for a variety of degrees and shapes of hearing loss in adults who are able to sit  
487 through a complete session. Then, because the responses and acquisition times may differ with infants  
488 (Werner et al., 1993), we will finally test the method for evaluating hearing thresholds in infants.

489 Clinical implementation of the pABR also requires calibration of the pABR stimuli using perceptual  
490 thresholds. Perceptual thresholds to the brief pABR stimuli show some temporal integration with increasing  
491 rate (Figures 6, 7), but less than full integration. The energy increases nearly 6-fold – or 8 dB – from a  
492 stimulation rate of 20 to 120 Hz, but the differences in perceptual thresholds ranged from 3.5 dB for the  
493 8000 Hz tone pip to 6 dB for the 500 Hz tone pip (Figure 7, Table 3). This minimal change in thresholds,  
494 and thus correction factors, across stimulation rates makes a multiple-rate paradigm easy to implement in  
495 an effort to obtain thresholds in the fastest recording time. For the optimal rate of 40 Hz, our normative  
496 values of 15.1–19.4 dB nHL for ER-2 earphones (Table 3, bottom) are lower than most reported values of  
497 20–26 dB nHL for tone pips at similar stimulation rates (37.1–39.1 Hz, 41 Hz) using ER-3A inserts (Sharma  
498 et al., 2003; Stapells, 2010; Stapells and Oates, 1997). This holds even when we use our correction factors  
499 (Table 3, top) and convert to dB nHL using the RETSPLs for ER-3A inserts. This suggests that the pABR  
500 may require lower levels to obtain a response, but there are other variables that may contribute to these  
501 different norms. Primarily, our method adjusts for both temporal integration and the subject's pure-tone  
502 threshold, whereas these other norms do not correct for thresholds < 15–20 dB HL (Sharma et al., 2003;  
503 Stapells, 2010; Stapells and Oates, 1997). Our values are more similar to the 17–21 dB nHL values  
504 obtained using the similar method of subtracting the pure-tone threshold from the threshold to the tone pip  
505 (Gorga et al., 1993). Other variables that contribute to some minor variation in norms are final step sizes  
506 (here we used 5 dB, others have used 2 dB), duration of the stimuli (like our study, most use 5 cycles, but  
507 some use 4 cycles), and calibration units for the tone pips (dB pSPL, peSPL, ppeSPL). We have provided  
508 the correction values in dB (Table 3, top) from which our normative dB nHL values were calculated, so that  
509 our values can be used by future studies by simply adding the RETSPLs for the transducers being used to  
510 the correction factors. We recommend using our correction factors because they directly compare our  
511 subjects' thresholds to pure-tones and tone pips while using the same transducer, thereby accounting for  
512 temporal integration, hearing threshold re: 0 dB HL, and transducer. When using different transducers for  
513 future studies, however, it is important to note that the frequency responses of earphones differ, which may  
514 affect the morphology and amplitudes of the pABR responses to high-frequency tone pips in particular. For  
515 example, ER-3A inserts are commonly used in the clinical systems, which have a spectrum that decreases



516 after 8 kHz. This is appropriate as most clinical diagnostic exams only test up to 4 kHz. But the pABR as  
517 implemented here tests up to 8 kHz, so we use the ER-2 inserts that have a flatter spectrum to 10 kHz.  
518 These differences in ER-2 and ER-3A transducer spectra have resulted in differences in ABRs to chirp  
519 stimuli (Elberling et al., 2012). Finally, these correction and normative values are for perception. Often,  
520 higher dB nHL levels are needed to evoke an electrophysiological response, and additional correction  
521 factors are needed to convert the physiological dB nHL level to estimated perceptual level (dB eHL). For  
522 example, for some systems, a normal hearing threshold of 25 dB eHL is established if an ABR response is  
523 present at 35–40 dB nHL for 500 Hz but 25 dB nHL for 4 kHz (American Academy of Audiology, 2012; BC  
524 Early Hearing Program, 2012; Ontario Ministry of Children, Community and Social Services, 2018). Now  
525 that we have established the dB nHL corrections, our next step is to determine the relationship between dB  
526 nHL and dB eHL thresholds for a range of hearing loss severities and configurations.

527 For this study we focused on the wave V component of the pABR responses. However, additional earlier  
528 ABR and later middle-latency components are visible in the responses to pABR stimuli, particularly in at the  
529 higher intensity of 81 dB peSPL (Figures 1, 4). While not quantified herein, measuring the earlier waves  
530 may provide useful information for other clinical and research applications, such as evaluating cochlear  
531 synaptopathy (Bharadwaj et al., 2014; Bramhall et al., 2017; Liberman et al., 2016; Prendergast et al.,  
532 2017). Perhaps measuring responses at a low and high rate may reveal differences in synchronization at  
533 different stages of early auditory processing (Milloy et al., 2017). Often clicks of higher intensity (>100 dB  
534 peSPL) are used but even 81 dB peSPL yields robust responses with the pABR. Furthermore, results from  
535 our earlier work suggest that the pABR may be more place-specific at higher intensities than serially  
536 presented stimuli (Polonenko and Maddox, 2019). Future studies can investigate the utility of the pABR for  
537 other application than estimating hearing thresholds.

## 538 5. Conclusions

539 The pABR evokes robust responses across a range of rates and intensities within reasonable recording  
540 times. The random timing affords extended analysis windows, allowing better estimates of noise in the pre-  
541 stimulus interval and faster detection of broader responses to low frequency tone pips or responses at  
542 lower intensities. A pABR method utilizing multiple stimulation may be useful in quickly estimating  
543 thresholds, particularly when thresholds are elevated at high but not low frequencies. We recommend that  
544 testing start with a stimulation rate of 40 Hz and a 10 ms analysis window. If responses are visible but  
545 longer times are needed to reach stopping criterion, then we suggest first increasing the analysis window to  
546 30 ms and then change the rate as necessary. For calibration, we recommended using the correction  
547 factors established here and then adding the appropriate RETSPL for the specific transducer, so that the  
548 norms account for temporal integration, pure-tone threshold, and transducer. Finally, our future studies will  
549 evaluate the relationship between the ABR and perceptual thresholds as well as the measurement time in  
550 a clinical setting.

## 551 Acknowledgments

552 This work was supported by National Institute for Deafness and Other Communication Disorders  
553 (R00DC014288, R01DC017962) awarded to RKM.

## 554 Declaration of interest

555 None.

## 556 Author contributions

557 **Melissa Polonenko:** Conceptualization, Data curation, Formal analysis, Investigation, Methodology,  
558 Project administration, Software, Validation, Visualization, Writing – original draft, review & editing

559 **Ross Maddox:** Conceptualization, Funding acquisition, Methodology, Resources, Software, supervision,  
560 Writing – review & editing

## 561 Data availability

562 EEG data will be made available in the EEG-BIDS format (Pernet et al., 2019) on Dryad (insert DOI when  
563 available), as well as the stimulus files and python code necessary to derive the pABR responses. The  
564 behavioral data are deposited to the same Dryad repository.

## 565 Supplemental material

566 The supplementary document provides the CDFs for all rates and intensities (Supplemental Figures 1 and  
567 2), as well as details of the linear mixed effects models for wave V latency and amplitude that include the  
568 gender variable (Supplemental Table 1).

## 569 References

- 570 American Academy of Audiology, 2012. Audiologic Guidelines for the Assessment of Hearing in Infants and  
571 Young Children. American Speech-Language-Hearing Association, Reston, VA.
- 572 Bates, D., Mächler, M., Bolker, B., Walker, S., 2015. Fitting Linear Mixed-Effects Models Using lme4. *J Stat*  
573 *Softw* 67, 1–48.
- 574 BC Early Hearing Program, 2012. Audiology assessment protocol.
- 575 Bharadwaj, H.M., Verhulst, S., Shaheen, L., Liberman, M.C., Shinn-Cunningham, B.G., 2014. Cochlear  
576 neuropathy and the coding of supra-threshold sound. *Front. Syst. Neurosci.* 8.  
577 <https://doi.org/10.3389/fnsys.2014.00026>
- 578 Bramhall, N.F., Konrad-Martin, D., McMillan, G.P., Griest, S.E., 2017. Auditory Brainstem Response  
579 Altered in Humans with Noise Exposure Despite Normal Outer Hair Cell Function. *Ear and Hearing*  
580 38, e1–e12. <https://doi.org/10.1097/AUD.0000000000000370>
- 581 Burkard, R., Hecox, K., 1983. The effect of broadband noise on the human brainstem auditory evoked  
582 response. I. Rate and intensity effects. *The Journal of the Acoustical Society of America* 74, 1204–  
583 1213. <https://doi.org/10.1121/1.390024>
- 584 Burkard, R., Shi, Y., Hecox, K.E., 1990. A comparison of maximum length and Legendre sequences for the  
585 derivation of brain-stem auditory-evoked responses at rapid rates of stimulation. *The Journal of the*  
586 *Acoustical Society of America* 87, 1656–1664. <https://doi.org/10.1121/1.399413>
- 587 Carhart, R., Jerger, J.F., 1959. Preferred Method For Clinical Determination Of Pure-Tone Thresholds.  
588 *Journal of Speech and Hearing Disorders* 24, 330–345. <https://doi.org/10.1044/jshd.2404.330>
- 589 Chiappa, K.H., Gladstone, K.J., Young, R.R., 1979. Brain Stem Auditory Evoked Responses: Studies of  
590 Waveform Variations in 50 Normal Human Subjects. *Arch Neurol* 36, 81–87.  
591 <https://doi.org/10.1001/archneur.1979.00500380051005>
- 592 Ching, T.Y.C., Day, J., Van Buynder, P., Hou, S., Zhang, V., Seeto, M., Burns, L., Flynn, C., 2014.  
593 Language and speech perception of young children with bimodal fitting or bilateral cochlear  
594 implants. *Cochlear Implants Int* 15 Suppl 1, S43-46.  
595 <https://doi.org/10.1179/1467010014Z.000000000168>
- 596 Cullington, H.E., Bele, D., Brinton, J.C., Cooper, S., Daft, M., Harding, J., Hatton, N., Humphries, J.,  
597 Lutman, M.E., Maddocks, J., Maggs, J., Millward, K., O'Donoghue, G., Patel, S., Rajput, K.,  
598 Salmon, V., Sear, T., Speers, A., Wheeler, A., Wilson, K., 2017. United Kingdom national paediatric  
599 bilateral project: Demographics and results of localization and speech perception testing. *Cochlear*  
600 *Implants International* 18, 2–22. <https://doi.org/10.1080/14670100.2016.1265055>
- 601 Don, M., Allen, A.R., Starr, A., 1977. Effect of Click Rate on the Latency of Auditory Brain Stem Responses  
602 in Humans. *Ann Otol Rhinol Laryngol* 86, 186–195. <https://doi.org/10.1177/000348947708600209>
- 603 Elberling, C., Kristensen, S.G.B., Don, M., 2012. Auditory brainstem responses to chirps delivered by  
604 different insert earphones. *J Acoust Soc Am* 131, 2091–2100. <https://doi.org/10.1121/1.3677257>
- 605 Elberling, C., Wahlgreen, O., 1985. Estimation of Auditory Brainstem Response, Abr, by Means of  
606 Bayesian Inference. *Scandinavian Audiology* 14, 89–96.  
607 <https://doi.org/10.3109/01050398509045928>
- 608 Eysholdt, U., Schreiner, C., 1982. Maximum length sequences -- a fast method for measuring brain-stem-  
609 evoked responses. *Audiology* 21, 242–250. <https://doi.org/10.3109/00206098209072742>
- 610 Gorga, M.P., Beauchaine, K.A., Reiland, J.K., Worthington, D.W., Javel, E., 1984. The effects of stimulus  
611 duration on ABR and behavioral thresholds. *The Journal of the Acoustical Society of America* 76,  
612 616–619. <https://doi.org/10.1121/1.391158>

- 613 Gorga, M.P., Kaminski, J.R., Beauchaine, K.L., Bergman, B.M., 1993. A Comparison of Auditory Brain  
614 Stem Response Thresholds and latencies Elicited by Air- and Bone-Conducted Stimuli. *Ear and*  
615 *Hearing* 14, 85–94.
- 616 Gorga, M.P., Thornton, A.R., 1989. The choice of stimuli for ABR measurements. *Ear Hear* 10, 217–230.  
617 <https://doi.org/10.1097/00003446-198908000-00002>
- 618 Gramfort, A., Luessi, M., Larson, E., Engemann, D.A., Strohmeier, D., Brodbeck, C., Goj, R., Jas, M.,  
619 Brooks, T., Parkkonen, L., Hämäläinen, M., 2013. MEG and EEG data analysis with MNE-Python.  
620 *Front. Neurosci.* 7. <https://doi.org/10.3389/fnins.2013.00267>
- 621 Green, P., MacLeod, C.J., 2016. SIMR: an R package for power analysis of generalized linear mixed  
622 models by simulation. *Methods in Ecology and Evolution* 7, 493–498. [https://doi.org/10.1111/2041-](https://doi.org/10.1111/2041-210X.12504)  
623 [210X.12504](https://doi.org/10.1111/2041-210X.12504)
- 624 Jiang, Z.D., Wu, Y.Y., Wilkinson, A.R., 2009. Age-related changes in BAER at different click rates from  
625 neonates to adults. *Acta Paediatr.* 98, 1284–1287. [https://doi.org/10.1111/j.1651-](https://doi.org/10.1111/j.1651-2227.2009.01312.x)  
626 [2227.2009.01312.x](https://doi.org/10.1111/j.1651-2227.2009.01312.x)
- 627 Kuznetsova, A., Brockhoff, P.B., Christensen, R.H.B., 2017. lmerTest Package: Tests in Linear Mixed  
628 Effects Models. *Journal of Statistical Software* 82, 1–26. <https://doi.org/10.18637/jss.v082.i13>
- 629 Larson, E., McCloy, D., Maddox, R., Pospisil, D., 2014. expyfun: Python experimental paradigm functions,  
630 version 2.0.0. Zenodo. <https://doi.org/10.5281/zenodo.11640>
- 631 Lasky, R.E., 1997. Rate and adaptation effects on the auditory evoked brainstem response in human  
632 newborns and adults. *Hearing Research* 111, 165–176. [https://doi.org/10.1016/S0378-](https://doi.org/10.1016/S0378-5955(97)00106-8)  
633 [5955\(97\)00106-8](https://doi.org/10.1016/S0378-5955(97)00106-8)
- 634 Lasky, R.E., 1984. A developmental study on the effect of stimulus rate on the auditory evoked brain-stem  
635 response. *Electroencephalogr Clin Neurophysiol* 59, 411–419. [https://doi.org/10.1016/0168-](https://doi.org/10.1016/0168-5597(84)90042-x)  
636 [5597\(84\)90042-x](https://doi.org/10.1016/0168-5597(84)90042-x)
- 637 Laukli, E., Burkard, R., 2015. Calibration/Standardization of Short-Duration Stimuli. *Semin Hear* 36, 3–10.  
638 <https://doi.org/10.1055/s-0034-1396923>
- 639 Liberman, M.C., Epstein, M.J., Cleveland, S.S., Wang, H., Maison, S.F., 2016. Toward a Differential  
640 Diagnosis of Hidden Hearing Loss in Humans. *PLOS ONE* 11, e0162726.  
641 <https://doi.org/10.1371/journal.pone.0162726>
- 642 Luts, H., Desloovere, C., Wouters, J., 2006. Clinical Application of Dichotic Multiple-Stimulus Auditory  
643 Steady-State Responses in High-Risk Newborns and Young Children. *AUD* 11, 24–37.  
644 <https://doi.org/10.1159/000088852>
- 645 Maddox, R.K., Lee, A.K.C., 2018. Auditory Brainstem Responses to Continuous Natural Speech in Human  
646 Listeners. *eNeuro* 5. <https://doi.org/10.1523/ENEURO.0441-17.2018>
- 647 May-Mederake, B., 2012. Early intervention and assessment of speech and language development in  
648 young children with cochlear implants. *Int J Pediatr Otorhinolaryngol* 76, 939–946.  
649 <https://doi.org/10.1016/j.ijporl.2012.02.051>
- 650 Milloy, V., Fournier, P., Benoit, D., Noreña, A., Koravand, A., 2017. Auditory Brainstem Responses in  
651 Tinnitus: A Review of Who, How, and What? *Front. Aging Neurosci.* 9.  
652 <https://doi.org/10.3389/fnagi.2017.00237>
- 653 Moeller, M.P., 2000. Early Intervention and Language Development in Children Who Are Deaf and Hard of  
654 Hearing. *Pediatrics* 106, e43–e43. <https://doi.org/10.1542/peds.106.3.e43>
- 655 NHS Newborn Hearing Screening Programme, 2013. Guidelines for the early audiological assessment and  
656 management of babies referred from the Newborn Hearing Screening Programme.
- 657 Niparko, J.K., Tobey, E.A., Thal, D.J., Eisenberg, L.S., Wang, N.-Y., Quittner, A.L., Fink, N.E., 2010.  
658 Spoken language development in children following cochlear implantation. *JAMA* 303, 1498–1506.  
659 <https://doi.org/10.1001/jama.2010.451>
- 660 Ontario Ministry of Children, Community and Social Services, 2018. Ontario Infant Hearing Program:  
661 Protocol for auditory brainstem response -based audiological assessment (ABRA), Version  
662 2018.01.
- 663 Pernet, C.R., Appelhoff, S., Gorgolewski, K.J., Flandin, G., Phillips, C., Delorme, A., Oostenveld, R., 2019.  
664 EEG-BIDS, an extension to the brain imaging data structure for electroencephalography. *Scientific*  
665 *Data* 6, 103. <https://doi.org/10.1038/s41597-019-0104-8>
- 666 Pittman, A.L., Stelmachowicz, P.G., 2003. Hearing loss in children and adults: Audiometric configuration,  
667 asymmetry, and progression. *Ear and hearing* 24, 198–205.  
668 <https://doi.org/10.1097/01.AUD.0000069226.22983.80>

- 669 Polonenko, M.J., Maddox, R.K., 2020. Exposing distinct subcortical components of the auditory brainstem  
670 response evoked by continuous naturalistic speech. *bioRxiv* 2020.08.20.258301.  
671 <https://doi.org/10.1101/2020.08.20.258301>
- 672 Polonenko, M.J., Maddox, R.K., 2019. The Parallel Auditory Brainstem Response. *Trends in Hearing* 23,  
673 2331216519871395. <https://doi.org/10.1177/2331216519871395>
- 674 Prendergast, G., Guest, H., Munro, K.J., Kluk, K., Léger, A., Hall, D.A., Heinz, M.G., Plack, C.J., 2017.  
675 Effects of noise exposure on young adults with normal audiograms I: Electrophysiology. *Hearing*  
676 *Research* 344, 68–81. <https://doi.org/10.1016/j.heares.2016.10.028>
- 677 R Core Team, 2020. R: A language and environment for statistical computing. R Foundation for Statistical  
678 Computing, Vienna, Austria.
- 679 Sharma, M., Purdy, S.C., Bonnici, L., 2003. Behavioural and Electroacoustic Calibration of Air-conducted  
680 Click and Toneburst Auditory Brainstem Response Stimuli. *Australian and New Zealand Journal of*  
681 *Audiology* 25, 54–60. <https://doi.org/10.1375/audi.25.1.54.31122>
- 682 Sininger, Y.S., Hunter, L.L., Hayes, D., Roush, P.A., Uhler, K.M., 2018. Evaluation of Speed and Accuracy  
683 of Next-Generation Auditory Steady State Response and Auditory Brainstem Response Audiometry  
684 in Children With Normal Hearing and Hearing Loss. *Ear and Hearing* 39, 1207–1223.  
685 <https://doi.org/10.1097/AUD.0000000000000580>
- 686 Stapells, D.R., 2010. Frequency-Specific ABR and ASSR Threshold Assessment in Young Infants. *A*  
687 *Sound Foundation through Early Amplification* 40.
- 688 Stapells, D.R., Oates, P., 1997. Estimation of the Pure-Tone Audiogram by the Auditory Brainstem  
689 Response: A Review. *AUD* 2, 257–280. <https://doi.org/10.1159/000259252>
- 690 Valderrama, J.T., de la Torre, A., Alvarez, I.M., Segura, J.C., Thornton, A.R.D., Sainz, M., Vargas, J.L.,  
691 2014. Auditory brainstem and middle latency responses recorded at fast rates with randomized  
692 stimulation. *The Journal of the Acoustical Society of America* 136, 3233–3248.  
693 <https://doi.org/10.1121/1.4900832>
- 694 Valderrama, J.T., de la Torre, A., Medina, C., Segura, J.C., Thornton, A.R.D., 2016. Selective processing  
695 of auditory evoked responses with iterative-randomized stimulation and averaging: A strategy for  
696 evaluating the time-invariant assumption. *Hearing Research* 333, 66–76.  
697 <https://doi.org/10.1016/j.heares.2015.12.009>
- 698 Van Maanen, A., Stapells, D.R., 2010. Multiple-ASSR Thresholds in Infants and Young Children with  
699 Hearing Loss. *Journal of the American Academy of Audiology* 21, 535–545.  
700 <https://doi.org/10.3766/jaaa.21.8.5>
- 701 Wang, T., Zhan, C., Yan, G., Bohórquez, J., Özdamar, Ö., 2013. A preliminary investigation of the  
702 deconvolution of auditory evoked potentials using a session jittering paradigm. *J. Neural Eng.* 10,  
703 026023. <https://doi.org/10.1088/1741-2560/10/2/026023>
- 704 Watson, C.S., Gengel, R.W., 1969. Signal Duration and Signal Frequency in Relation to Auditory  
705 Sensitivity. *The Journal of the Acoustical Society of America* 46, 989–997.  
706 <https://doi.org/10.1121/1.1911819>
- 707 Werner, L.A., Folsom, R.C., Mancl, L.R., 1993. The relationship between auditory brainstem response and  
708 behavioral thresholds in normal hearing infants and adults. *Hearing Research* 68, 131–141.  
709 [https://doi.org/10.1016/0378-5955\(93\)90071-8](https://doi.org/10.1016/0378-5955(93)90071-8)
- 710